

Measurement of Positronium hyperfine splitting with quantum oscillation

Y.Sasaki^a, A.Miyazaki^a, A.Ishida^a, T.Namba^a, S.Asai^a, T.Kobayashi^a, H.Saito^b, K.Tanaka^c, and A.Yamamoto^c

^aDepartment of Physics Graduate School of Science, and International Center for Elementary Particle Physics, University of Tokyo, Hongo, Bunkyo-ku, Tokyo 113-0033, Japan

^bDepartment of General Systems Studies, Graduate School of Arts and Sciences, The University of Tokyo, 3-8-1 Komaba, Meguro-ku, Tokyo, 153-8902, Japan

^cHigh Energy Accelerator Research Organization (KEK), 1-1 Oho, Tsukuba, Ibaraki, 305-0801, Japan

Abstract

Interference between different energy eigenstates in a quantum system results in an observable oscillation with a frequency which is proportional to the difference in energy between the states. Such an oscillation is observable in positronium when it is placed in a magnetic field. In order to measure the hyperfine splitting of positronium we perform the precise measurement of this oscillation using a high quality superconducting magnet and fast photon-detectors. A result of $203.324 \pm 0.039(\text{stat.}) \pm 0.015(\text{sys.})$ GHz is obtained which is consistent with both theoretical calculations and previous precision measurements. The relaxation of positronium spin is also discussed.

Keywords: QED, positronium, quantum oscillation

1. Introduction

Positronium (Ps), the bound state of an electron and a positron, is the lightest hydrogen-like atom. Since it is a purely leptonic system, and thus free from the uncertainties of hadronic interactions, it is an excellent object for studying Quantum Electro Dynamics(QED), especially for the bound-state. The two lowest energy states of Ps, a triplet state (1^3S_1) and a single state (1^1S_0), are known as orthopositronium(o-Ps) and parapositronium(p-Ps), respectively. The difference in the energy between o-Ps and p-Ps is called the HyperFine Splitting (HFS) (203 GHz) and it is significantly larger than that of the hydrogen-atom (1.4 GHz). A theoretical prediction including $O(\alpha^3)$ corrections has recently been obtained using the NRQED approach[1]. The result of this calculation deviates from the previously measured values[2, 3] by a significant margin (3.9σ , 15 ppm).

In a magnetic field the two states $|s = 1, m_z = 0\rangle$ and $|s = 0, m_z = 0\rangle$ mix to result in the states $|+\rangle$ and $|-\rangle$, where

$$|+\rangle = C_1^1|s = 1, m_z = 0\rangle + C_0^1|s = 0, m_z = 0\rangle, \quad (1)$$

$$|-\rangle = C_1^0|s = 1, m_z = 0\rangle + C_0^0|s = 0, m_z = 0\rangle, \quad (2)$$

and

$$C_1^0 = -C_0^1 = \left\{ \frac{1}{2} \left[1 - (1 + \chi^2)^{-\frac{1}{2}} \right] \right\}^{\frac{1}{2}}, \quad (3)$$

$$C_1^1 = C_0^0 = \left\{ \frac{1}{2} \left[1 + (1 + \chi^2)^{-\frac{1}{2}} \right] \right\}^{\frac{1}{2}}. \quad (4)$$

On the other hand $|s = 1, m_z = \pm 1\rangle$ states do not couple with the static magnetic field and so remain unperturbed. The energy split between $|+\rangle$ and $|s = 1, m_z = \pm 1\rangle$ (the Zeeman split) is

$$\Delta_{\text{mix}} = \frac{\Delta_{\text{HFS}}}{2} (\sqrt{1 + \chi^2} - 1), \quad (5)$$

where $\chi = \frac{2g'\mu_B H}{\Delta_{\text{HFS}}}$, H is the static magnetic field strength, Δ_{HFS} is the HFS without the magnetic field, μ_B is the Bohr magneton and $g' = g(1 - \frac{5}{24}\alpha^2)$ is the g factor of an electron(positron) with a bound-state correction[2]. Since χ is small in a weak magnetic field, Δ_{mix} is approximately proportional to the HFS.

In all of the previous experiments the value of the HFS is obtained via the above formula by measuring the Zeeman splitting in a magnetic field of a known strength [5]. There are two distinct approaches for measuring the Zeeman split. The first approach uses an external high power light source with a resonant frequency of Δ_{mix} (about 3 GHz in a magnetic field of ≈ 8 kGauss) to stimulate the transition $|s = 1, m_z = \pm 1\rangle$ to $|+\rangle$. This method has been used in many previous experiments, for example Mills [2] and Ritter [3], and has resulted in measurements with accuracies of $O(1)$ ppm. The second approach as proposed by V.G.Baryshevsky [4] makes use of the quantum oscillation between $|s = 1, m_z = \pm 1\rangle$ and $|+\rangle$. This oscillation was observed by him in a subsequent experiment[6]. Positrons emitted from a β^+ source are polarized in the direction of their momentum due to parity violation in the weak interaction. (The polarization ratio P is determined by the initial velocity β of the positron, $P = \beta$). Consequentially the resultant o-Ps is also highly polarized. This o-Ps is a superposed state of $|+\rangle$ and $|s = 0, m_z = \pm 1\rangle$ and the superposition oscillates with a frequency which is proportional to Δ_{mix} . In 1996, S.Fan [7] performed an improved experiment using this quantum oscillation method, obtaining a result of 202.5 ± 3.5 GHz. This result still has an accuracy worse than 1%.

In this paper we greatly improve the accuracy of the measurement using the quantum oscillation method by using a very high quality magnetic field and a fast photon-detection system. This method is based on the spin rotation of o-Ps (Ps-SR). It is interesting to note that using the relaxation of o-Ps spin, Ps-SR

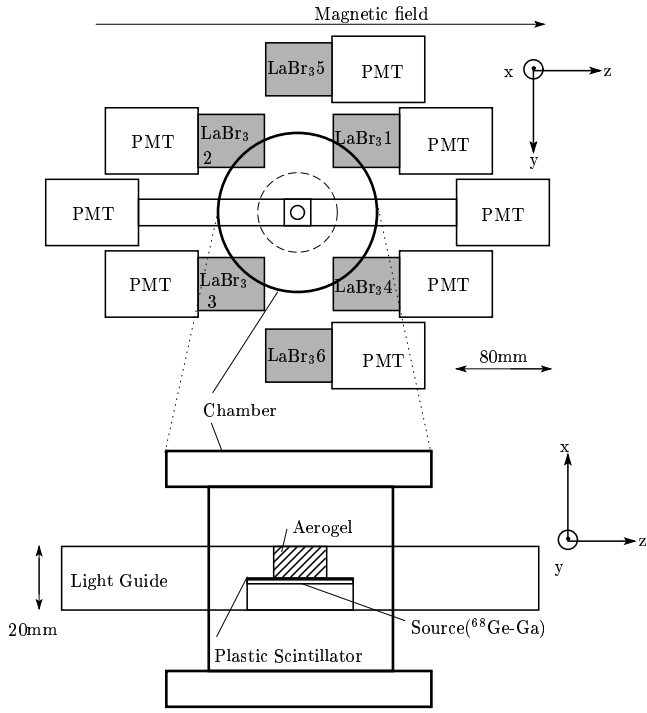


Figure 1: Schematic diagram of the experimental setup. The upper figure shows the entire experimental setup. The magnetic field direction is along the z -axis and the $\text{LaBr}_3(\text{Ce})$ scintillators are placed in the yz -plane. The direction of the β^+ emitted from the $^{68}\text{Ge-Ga}$ source is along the x -axis. The bold circle is the Ps chamber. The coordinate system is also shown. The lower figure is a magnified view of the Ps chamber, in which the $^{68}\text{Ge-Ga}$ source, the thin plastic scintillator and the Aerogel are located.

can be used for probing various materials in material science research [8]. Since Ps is much lighter than a muon, the relaxation processes of Ps spin are expected to be much more sensitive than those from μ -SR, (unfortunately the lifetime of o-Ps is much shorter than that of a muon).

2. Experimental setup

The upper figure of Figure 1 shows a schematic diagram of the experimental setup, while the lower figure shows a magnified view of the Ps chamber. The coordinate system is defined in both of these figures. A $^{68}\text{Ge-Ga}$ positron source (30 kBq) with an end point energy of 1.9 MeV is used as a β^+ source. A positron passes through the plastic scintillator (NE102, thickness=500 μm), and the resulting two light pulses are transmitted in either direction by the light guide to two photomultipliers (PMT: Hamamatsu R5924-70). The positron then goes on to form Ps in the silica aerogel target (SiO_2 ; 10 mm in diameter \times 10 mm length, density 0.11 g/cm^3 , the surface of the primary grain is made hydrophobic in order to avoid the electric dipole of OH-). The plastic scintillator tags the positron emitted along the direction of the x -axis which results in the o-Ps being polarized along the x -axis. The entire Ps system is contained within a chamber evacuated to 1×10^{-2} Torr in order to reduce pick-off annihilation.

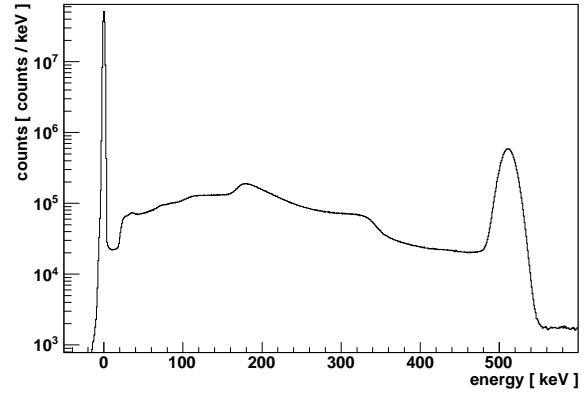


Figure 2: Energy spectrum of a LaBr_3 crystal measured in the magnetic field of 100 mT.

The magnetic field (z -direction) is provided by a superconducting magnet which was originally developed for medical NMR use. It has a large bore size (80 cm) and an excellent uniformity of 10 ppm over the volume of the silica aerogel. The magnetic field is measured with an NMR magnetometer (ECHO-ELECTRONICS, EFM-150HM-AX) which has a calibration uncertainty of 35 ppm.

The produced o-Ps decays into three gammas, and the gamma-rays are detected by six LaBr_3 crystals (1.5 inches in diameter \times 2 inches length. PMT:Hamamatsu R5924-70). The LaBr_3 detectors are located at $(\theta, \phi) = (\frac{\pi}{4}, -\frac{\pi}{2}), (\frac{3\pi}{4}, -\frac{\pi}{2}), (\frac{3\pi}{4}, \frac{\pi}{2}), (\frac{\pi}{4}, \frac{\pi}{2}), (\frac{\pi}{2}, -\frac{\pi}{2}), (\frac{\pi}{2}, \frac{\pi}{2})$, where $\theta = \arccos(\frac{z}{\sqrt{x^2+y^2+z^2}})$ and $\phi = \arctan(\frac{y}{x})$. The detectors will be referred to by the indices 1 ~ 6 respectively, and each of the detectors is labelled accordingly in Figure 1. The quantum oscillation modulates the angular distribution of the three gammas emitted from the o-Ps decay and the decay curve of o-Ps beats with this oscillation. Unlike the muon precession, in which the emission direction of $\mu \rightarrow e$ rotates, this oscillation changes its angular distribution as a “vibration” in the yz -plane. This is a unique property of a spin-1 system. The 1st and 3rd detector pair observes the oscillation with the same phase while the 2nd and 4th detector pair observes the inverse phase. The 5th and 6th detectors observe the exponential decay curve without the oscillation.

Figure 2 shows the energy spectrum measured with the LaBr_3 crystals. We note that a good energy resolution of 4.0 % (FWHM) at 511 keV is obtained, even with the photomultipliers located within a magnetic field of 100 mT. The time resolution of the LaBr_3 detectors is 200 ps (FWHM) for the 511 keV gamma peak and the time resolution of the positron tagging plastic scintillator is 3.8 ns(FWHM). These measurements were also obtained with the photomultipliers within the magnetic field.

Data acquisition is started(740 Hz) when the plastic scintillator signal is coincident within -50 ns to 1650 ns with at least one of the LaBr_3 signals. “ $t=0$ ” is defined as the timing of the plastic scintillator pulse. A charge ADC (CAEN C1205) is used

to measure the energy information of the LaBr₃ crystals while another charge ADC (REPIC RPC-022) is used to measure both the base-line information of the LaBr₃ crystals and the energy information of the plastic scintillator. The charge is measured just before the gamma-ray arrives at the LaBr₃ crystal (base-line information) in order to remove pile-up events. The time differences between the plastic scintillator and LaBr₃ scintillators are measured by direct clock TDCs (5 GHz:time resolution of 200 psec). These TDCs have excellent integral and differential linearities.

Separate measurements have been made for 5 different magnetic field strengths: 0 mT, 100 mT, 118 mT, 135 mT and 138 mT. Also, both +z and -z polarization measurements were performed by changing the direction of emission of the β^+ . The expected time periods of the oscillation are about 26 and 14 nsec for 100 mT and 138 mT, respectively. The period of each run was about 3 days and the total data acquisition period was about 22 days. 1.4×10^9 events were recorded. The energy and timing spectra were calibrated every hour using the prompt 511keV and pedestal peaks.

3. Analysis

The following event selections are applied in order to obtain a clean time spectrum;

1. In order to remove pile-up events, the fluctuation of the base-line of the LaBr₃ is required to be smaller than 3σ (where σ is the noise level).
2. The events for which more than two LaBr₃ crystals are hit simultaneously are disregarded. This helps to reduce the accidental contribution since accidental events have a back-to-back topology.
3. In order to obtain a good time resolution, the energy deposited in the LaBr₃ is required to be larger than 100 keV.

Since the multiple hit events are removed, six statistically independent time spectra are thus obtained. We then fit the spectra using two distinct methods: the “separate fitting method” and the “subtracting method”

3.1. Separate fitting method

Figures 3 show the timing spectra with the best fit result using the separate fitting method. For this method the six time spectra are simultaneously fit in the range 50 ns to 1450 ns with the following function:

$$\begin{aligned}
 f_n(t) &= A_n e^{-\gamma_1 t} + B_n e^{-\gamma_2 t} \\
 &+ C_n e^{-\frac{\gamma_1 + \gamma_2}{2} t} \times \sin(\Omega t + \theta_n) \\
 &+ D_n
 \end{aligned} \tag{6}$$

for $n = 1, 2, 3, 4$

$$\begin{aligned}
 f_n(t) &= A_n e^{-\gamma_1 t} + B_n e^{-\gamma_2 t} \\
 &+ D_n
 \end{aligned} \tag{7}$$

for $n = 5, 6$

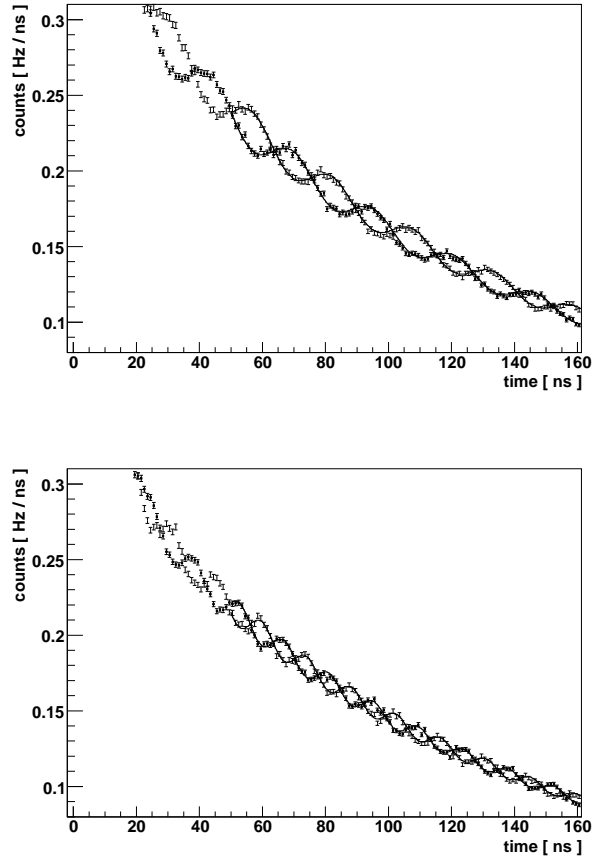


Figure 3: The timing spectra at 100 mT(upper) and 135 mT(lower). In both figures, data are plotted with error bars and the solid lines show the best fit results. The opposite phase spectra are superimposed in both figures and the polarization direction of β^+ is upwards.

where n denotes the LaBr₃ detector index and $\Omega = \Delta_{\text{mix}}/\hbar$. The two decay rates γ_1, γ_2 and the angular frequency of the oscillation Ω are defined as common variables, while the others are completely free. γ_1 and γ_2 are decay rates for $|s = 1, m_z = \pm 1\rangle$ and $|+\rangle$. These rates include the effect of pick-off annihilation.

The results of the fits for LaBr₃ 1 are listed in Table 1 for the 100 mT case. All fitted variables converged as shown in the table, and a reasonable χ^2/ndf of 1.00 is obtained. The fitted lifetime values are 136.4 ± 2.2 nsec and 102.5 ± 2.5 nsec, which are consistent with the lifetime ($|s = 1, m_z = \pm 1\rangle$) measured in aerogel [9] and the calculated value ($|+\rangle$) in a magnetic field of 100 mT, respectively. A fitted time period ($2\pi/\Omega$) of 25.57 ± 0.02 nsec(700 ppm) is obtained for this run.

The same procedure is applied for the runs with different magnetic field strengths and different polarizations. The resultant χ^2/ndf 's were always found to be less than 1.03. The fitted Ω is proportional to Δ_{mix} and Δ_{HFS} can be calculated using formula(1). The obtained Δ_{HFS} are listed in Table 2 for the various magnetic field strengths.

The 118mT (up polarization) measurement was also performed using a different TDC clock(8 GHz) and consistent results were obtained. This is an important check for the TDC,

Table 1: An example of the results of a spectra fit using the “separate fitting method” (100 mT(up))

Parameter	Fitting
A_1	0.095 ± 0.011
B_1	0.078 ± 0.012
C_1	0.0096 ± 0.0003
D_1	0.00733 ± 0.00001
θ_1	0.18 ± 0.03
γ_1	0.00733 ± 0.00012
γ_2	0.00975 ± 0.00024
Ω	0.24573 ± 0.00017
χ^2/ndf	$1.00 (ndf=8370)$

Table 2: Summary of the HFS values obtained using the “separate fitting method”. “up” and “down” denote the direction of the β^+ with respect to the x -axis. “TDC” denotes the run for which a different TDC clock was used.

Run	Magnetic Field [mT]	HFS [GHz]
100mT(down)	100.592	203.04 ± 0.12
100mT(up)	100.594	203.17 ± 0.14
118mT(down)	118.824	203.42 ± 0.19
118mT(up)	118.826	203.14 ± 0.21
118mT(up,TDC)	118.826	203.63 ± 0.23
135mT(down)	134.805	203.58 ± 0.11
135mT(up)	134.807	203.26 ± 0.14
138mT(down)	138.326	203.45 ± 0.14
138mT(up)	138.330	203.37 ± 0.12

since the time spectrum is crucial for this experiment.

The Δ_{HFS} values obtained at the various magnetic field strengths are consistent with each other. The combined value is 203.336 ± 0.048 (stat.) GHz.

3.2. Subtracting method

For this method the sum of the 2nd and 4th spectra are subtracted from the sum of the 1st and 3rd spectra. Ideally this would cancel the exponential components in the spectra, leaving only the oscillating component. Unfortunately the acceptances of the LaBr₃ detectors are not exactly the same which results in small exponential components remaining after the subtraction. These components are thus still included in the fit, but the upshot is that the oscillating component is greatly enhanced. Furthermore, the cancellation of the prompt peak means that the fitting region can be extended closer to zero resulting in a smaller statistical error in the fit. Figures 4 shows examples of subtracted time spectra with the best fits superimposed. The fitting region is set from 16 ns to 1416 ns and the following formula is used:

$$\begin{aligned}
 f(t) &= Ae^{-\gamma_1 t} + Be^{-\gamma_2 t} \\
 &+ Ce^{-\frac{\gamma_1 + \gamma_2}{2} t} \times \sin(\Omega t + \theta) \\
 &+ D
 \end{aligned} \tag{8}$$

The two exponential components with proportionality constants A and B are for the remnant decay curves, while the

Table 3: An example of the results of a spectra fit using the “subtracting method” (100 mT(up))

Parameter	Fitting
A	0.0056 ± 0.0042
B	-0.0015 ± 0.0043
C	0.0377 ± 0.0008
D	0.00013 ± 0.00002
γ_1	0.0077 ± 0.0010
γ_2	0.0094 ± 0.0010
Ω	0.24558 ± 0.00014
θ	0.16 ± 0.02
χ^2/ndf	$1.00 (ndf=1392)$

Table 4: Summary of the HFS values obtained using the “subtracting method”. “up” and “down” denote the direction of the β^+ with respect to the x -axis. “TDC” denotes the run for which a different TDC clock was used.

Run	Magnetic Field [mT]	HFS [GHz]
100mT(down)	100.592	203.11 ± 0.10
100mT(up)	100.594	203.30 ± 0.12
118mT(down)	118.824	203.38 ± 0.16
118mT(up)	118.826	203.15 ± 0.17
118mT(up,TDC)	118.826	203.55 ± 0.18
135mT(down)	134.805	203.46 ± 0.09
135mT(up)	134.807	203.27 ± 0.11
138mT(down)	138.326	203.42 ± 0.11
138mT(up)	138.330	203.34 ± 0.09

component with constant C is the oscillation contribution. The amplitudes A, B and D are expected to be small.

The fitted results are listed in Table 3 for the 100 mT case. The coefficients A,B are consistent with zero and D is also much smaller than C, which means that the cancellation works well. A fitted time period($2\pi/\Omega$) of 25.59 ± 0.01 nsec(590ppm) is obtained for this run.

The obtained Δ_{HFS} are listed in Table 4 for the various magnetic field strengths. The Δ_{HFS} values obtained at the various magnetic field strengths are consistent with each other. The combined value is 203.324 ± 0.039 (stat.) GHz.

4. Discussion and Result

4.1. Systematic errors

The systematic errors are summarized below:

1. Varying the frequency sweep range of the NMR magnetometer resulted in slightly different readings. The uncertainty in the magnetometer calibration was estimated from this deviation (35ppm).
2. Non-uniformity of the magnetic field results in the following two effects: (1) The oscillations in the time spectra become smeared. This effect is already taken into account in the statistical errors listed in Table 2 and 4. (2) There may be a difference between the value of the magnetic field strength as measured by the NMR, and the actual values over the range of the aerogel. This effect is estimated at 10ppm.

3. The accuracy of the TDC is determined by the accuracy of the clock (Hittite, HMC-T2000), which is better than 2ppm. The effects of differential and integrated non-linearities in the TDC are negligible.
4. The fitting region dependence is negligible as long as the fitting start time is later than 50 nsec for the separate fitting method, and 16 ns for the subtracting method.

Since Δ_{HFS} depends on the magnetic field squared, systematic errors due to the magnetic field uncertainty are doubled. Systematic errors are combined in quadrature.

4.2. Discussion

$$\Delta_{\text{HFS}} =$$

$$203.336 \pm 0.048(\text{stat.}) \pm 0.015(\text{sys.}) \text{ GHz (separate fitting)}$$

$$203.324 \pm 0.039(\text{stat.}) \pm 0.015(\text{sys.}) \text{ GHz (subtracting)}$$

We note that the results of the two different fitting methods are consistent. We use the more accurate subtracting method value as the final result. The accuracy is 200 ppm, which is an improvement by a factor 90 over the previous experiment which used the oscillation method[7]. This result is consistent with both the theoretical calculation[1] and the previous more-precise experimental values which directly measure the Zeeman transition[2, 3].

In order to observe the relaxation of Ps spin (Ps-SR), the oscillation amplitude was fitted as a function of time, but the result is consistent with a constant. A better accuracy and a higher density target are necessary to observe the relaxation.

The accuracy of the measured HFS value for this study is 200 ppm. The following four points can be improved to achieve a better accuracy:

- (1) Increase the total run time by a factor 20 (about 1.5 years).
 - (2) Increase the intensity of the radioactive source by a factor 3. The dead time of the DAQ would still be acceptable.
 - (3) Increase the coverage of the photon detectors by a factor 3. Fine segmentation is still necessary.
 - (4) The absolute calibration of the NMR and the uniformity of the magnetic field can both easily be improved to $O(1)$ ppm.
- The result of these improvements would be an increase in statistics by a factor 180 and an improvement of the final accuracy to about 15 ppm.

We thank Dr.M.Ikeno(KEK) for the development of the TDC. Sincere gratitude is expressed to Mr. M.M.Hashimoto for the useful discussions.

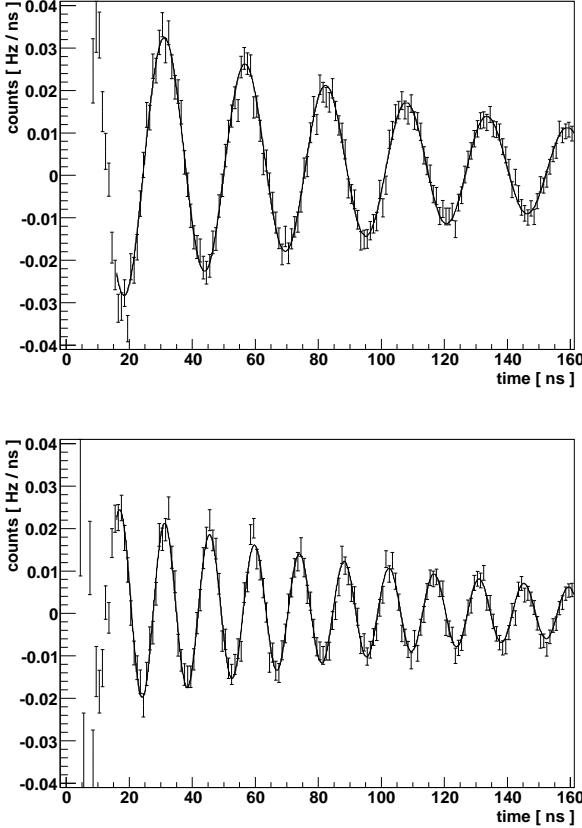


Figure 4: Time spectra after the “subtracting method” for B=100 mT(Upper) and 135 mT(Lower). In both figures, data are plotted with error bars and the solid lines show the best fit results.

References

- [1] G.S. Adkins, R.N. Fell, and P.M. Mitrikov., Phys. Rev. Lett. **79** (1997) 3383; B. kniehl and A.A. Penin, Phys. Rev. Lett., **85** (2000) 5094; K. Melnikov et.al., Phys. Rev. Lett. **86** (2001) 1498.
- [2] A.P. Mills, Phys. Rev. A **27** (1983) 262.
- [3] M.W. Ritter *et al.*, Phys. Rev. A **30** (1984) 1331.
- [4] V.G. Baryshevsky *et al.*, J. Phys. B **22** (1989) 2835.
- [5] New experimental approach without Zeeman effect has been proposed in S. Asai *et al.*, arXiv 0805.4672 (2008). The direct transition from o-Ps to p-Ps is made using the high power sub-THz light source.
- [6] V.G. Baryshevsky *et al.*, Phys. Rev. A **136** (1989) 428.
- [7] S. Fan *et al.*, Phys. Rev. A **216** (1996) 129.

- [8] E. Ivanov *et al.*, Nucl. Inst. Meth. A **267** (2009) 347.
- [9] Lifetime becomes shorter due to the pickoff collision with the aerogel
Y. Kataoka *et al.*, Phys. Lett. B. **671** (2009) 219; O. Jinnouchi *et al.*, Phys.
Lett. B. **572** (2003) 117; S. Asai *et al.*, Phys. Lett. B. **357** (1995) 475.